HHS Public Access

Author manuscript

Circ Cardiovasc Imaging. Author manuscript; available in PMC 2023 November 15.

Published in final edited form as:

Circ Cardiovasc Imaging. 2022 November ; 15(11): e014645. doi:10.1161/CIRCIMAGING.122.014645.

Optimal Echocardiographic Parameters to Improve the Diagnostic Yield of Tc-99m-Bone Avid Tracer Cardiac Scintigraphy for Transthyretin Cardiac Amyloidosis

Sarah AM Cuddy, MB BCh BAO[a,b], **Yesh Datar, BA**[a,b], **Gavin Ovsak, MD**[a], **Sunil Saith, MD**[e], **Sean Murphy, MB BCh BAO**[a], **Camden Bay, PhD**[c], **Mia Haddad, MPH**[a], **Brian Lilleness, MD**[d], **Varsha Muralidhar, MD**[d], **Alexandra Pipilas, MD**[d], **Jacqueline Vuong, MD**[d], **Eric Guardino, MD**[d], **Mathew S. Maurer, MD**[e], **Frederick L. Ruberg, MD**[d], **Rodney H Falk, MD**[a], **Sharmila Dorbala, MD MPH**[a,b,c]

[a]Cardiac Amyloidosis Program, Division of Cardiology, Department of Medicine, Brigham and Women's Hospital, Boston, Massachusetts

[b]CV imaging program, Cardiovascular Division and Department of Radiology, Brigham and Women's Hospital, Boston, Massachusetts

[c]Division of Nuclear Medicine, Department of Radiology, Brigham and Women's Hospital, Boston, Massachusetts

[d]Section of Cardiovascular Medicine, Department of Medicine, Boston University School of Medicine/Boston Medical Center, Boston, Massachusetts

[e]Division of Cardiology, Columbia University Irving Medical Center, New York, New York

Abstract

Background: Echocardiographic deformation-based ratios and novel multi-parametric scores have been suggested to discriminate transthyretin cardiac amyloidosis (ATTR-CM) from other causes of increased left ventricular wall thickness among patients referred for ATTR-CM evaluation. Their relative predictive accuracy has not been well studied. We sought to (1) identify echocardiographic parameters predictive of ATTR-CM and (2) compare the diagnostic accuracy of these parameters in patients with suspected ATTR-CM referred for technetium-99m-pyrophosphate (Tc-99m-PYP) scintigraphy.

Methods: Echocardiograms from 598 patients referred to three major amyloidosis centers for Tc-99m-PYP to detect ATTR-CM were analyzed, including longitudinal strain (LS) analysis. Deformation ratios [septal apex to base (SAB) ratio, relative apical sparing (RELAS), ejection fraction to global LS (EFSR)], a multi-center European increased wall thickness (IWT) score and Mayo Clinic derived ATTR score (TCAS) were calculated. A logistic regression model was used

Address for Correspondence: Sarah Cuddy, Brigham and Women's Hospital, 75 Francis Street, Boston, MA 02115. Scuddy1@bwh.harvard.edu, Phone: 617-732-8410.

Supplemental Materials:
Supplemental Method
Supplemental Results
Tables S1–S2
Figures S1

to identify the parameters that best associated with a diagnosis of ATTR-CM. Comparison of the diagnostic capacity of the parameters was performed by receiver operating characteristic curves and the area under the curve (AUC).

Results: Over half of the subjects (54.2%) were diagnosed with ATTR-CM [78% were male, median age of 76 years]. Age, inferolateral wall thickness, and basal LS were the strongest predictors of ATTR-CM, AUC of 0.87 (95% confidence interval (CI): 0.83, 0.90), superior to the IWT score AUC of 0.78 (95% CI: 0.73, 0.83; p=0.004). An inferolateral wall thickness of ≥ 14 mm (AUC 0.73) was as accurate as the published cut-offs for TCAS score and SAB (AUC: 0.72 & 0.69, p=0.8 & p=0.1, respectively), and was superior to EFSR and RELAS (AUC: 0.64 & 0.53, p<0.001, respectively). A cut-off of ≥−8% for average basal LS (AUC: 0.76, CI: 0.72–0.79) had a similar AUC to TCAS (p=0.2); outperforming the other indices (p<0.01).

Conclusions: Inferolateral wall thickness and average basal LS performed as well as or better than more complex echo ratios and multiparametric scores to predict ATTR-CM.

Keywords

Amyloidosis; Cardiomyopathy; Transthyretin; Echocardiography

Subject Terms:

Cardiomyopathy; Heart Failure; Diagnostic Testing; Echocardiography; Nuclear Cardiology and PET

INTRODUCTION

Cardiac amyloidosis most commonly results from extracellular deposits of transthyretin (ATTR-CM) or immunoglobulin light chain proteins in the heart. Echocardiography is the most common first investigation to raise the suspicion of cardiac amyloidosis. However, none of the echocardiographic features are definitive for diagnosing cardiac amyloidosis and in the past, histological confirmation was necessary. Historically, ATTR-CM was diagnosed by endomyocardial biopsy due to the low sensitivity of fat pad biopsy. More recently, the noninvasive diagnosis of ATTR-CM has been revolutionized by the repurposing of bone-avid radiotracers technetium-99m-labeled 3,3-diphosphono-1,2-propanodicarboxylicacid (DPD), hydroxymethylene diphosphonate (HDP), and pyrophosphate (PYP) for cardiac scintigraphy, negating the need for biopsy in patients without a monoclonal gammopathy.[1]

Echocardiography serves as a gatekeeper for referral to bone avid tracer cardiac scintigraphy. With more widespread use of bone avid tracer cardiac scintigraphy, the proportion of positive scans is declining. Appropriate selection of patients for bone avid tracer cardiac scintigraphy will be critical to maintain a high yield. Increased wall thickness, due to the extra-cellular deposition of amyloid fibrils, is a fundamental component of the pathogenesis of this disease. Infiltration also causes diastolic dysfunction leading to a restrictive left ventricular (LV) filling pattern. These features are readily detected by echo; however, they are not specific for ATTR-CM.[2] Speckle tracking echo allows detection of abnormal myocardial deformation, measured by longitudinal strain (LS),

and has a characteristic apical sparing pattern in cardiac amyloidosis, which has been shown to differentiate cardiac amyloidosis from other causes of increased ventricular wall thickness.[3] Several different strain based ratios have been devised to aid detection of cardiac amyloidosis; a ratio of LS at the apex divided by the mean of strain at mid-ventricle and base (RELAS)[3], a 4-chamber septal apical to base ratio (SAB)[4], and an ejection fraction to global LS ratio[5].

Given the multitude of echo features, combining them into a multiparametric score to increase the identification of true ATTR-CM is appealing. Recently, investigators have developed a score, using data from three European amyloidosis referral centers, referred to as the increased wall thickness (IWT) score[6]. The components of this score include relative wall thickness, E/e' ratio, LS, tricuspid annulus planar systolic excursion (TAPSE) and SAB. The Mayo clinic also developed a score entitled a transthyretin cardiac amyloidosis score (TCAS)[7], which comprises of age, sex, relative wall thickness, posterior wall thickness, left ventricular ejection fraction (EF), and history of hypertension. The comparative performance of either of these scores to identify ATTR-CM in external cohorts has not been studied.

Therefore, our aims were (1) to identify echo features that best predict ATTR-CM and (2) to compare and validate the value of echo measures, strain ratios, and multiparametric echo scores, for diagnosing ATTR-CM by positive Tc-99m-PYP SPECT. To address our aims, we compiled a large registry of patients with suspected ATTR-CM who underwent echocardiography and Tc-99m-PYP SPECT from three major centers with expertise in amyloidosis in the United States. This 3-site retrospective registry provided a large dataset to address these aims and offers key advantages to overcome differences in referral patterns and makes the results more generalizable than a single center study.

METHODS

The data that support the findings of this study are available from the corresponding author upon reasonable request. Patients who underwent both an echocardiogram and Tc-99m-PYP SPECT within a six-month interval and were seen between 2011 and 2020 at three centers: Brigham and Women's Hospital (BWH), Boston, MA; Boston University School of Medicine/Boston Medical Center (BMC), Boston, MA, and Columbia University Irving Medical Center/New York-Presbyterian Hospital (CUIMC/NYP), New York City, NY were evaluated retrospectively. The median interval between echocardiogram and Tc-99m-PYP SPECT in this cohort was 7 days. The exclusion criteria included non-ATTR amyloidosis; monoclonal gammopathy identified by immunofixation electrophoresis of serum or urine, and serum free light chain assay without a tissue biopsy; an uninterpretable echo; and unavailable clinical data. Tc-99m-PYP scintigraphy can be positive prior to clinical or echocardiographic manifestations of amyloidosis[8] and is used for screening of patients with TTR gene mutations; identifying pre-clinical cardiac involvement with or without neuropathy was beyond the scope of this study, hence, all hereditary ATTR subjects with non-V122I mutations were excluded, as well as patients with V122I mutation with both normal wall thickness and normal NT-proBNP. A total of 228 subjects were excluded from subsequent image analysis (Figure 1). The final cohort included 239, 152, 207 subjects from BWH, BMC, and CUIMC/NYP, respectively. This study was approved by the Brigham and

Women's Hospital Institutional Review Board, and the Institutional Review Boards of the collaborating sites. Due to the retrospective nature of the study, informed consent was not required.

Data collection

Clinical data was collected by chart review and included standard demographic variables; variables pertaining to a history of cardiovascular disease, tendinopathies, neuropathy; variables related to diagnostic work-up including biopsy results and standard laboratory tests. Myocardial uptake of Tc-99m-PYP on SPECT or SPECT/CT images were graded visually per the Perugini grading system comparing myocardial uptake to rib uptake of radiotracer (grade 0 =no myocardial uptake, and grades 1 to 3 as myocardial uptake < rib uptake, = rib uptake, and > rib uptake, respectively) at each site. Tc-99m-PYP grade 2 or 3 were recorded as positive scans for ATTR-CM and grade 0 or 1 as a negative scan for ATTR-CM in keeping with the prior and current guidelines. No cases were diagnosed using planar heart to contralateral (H:CL) ratio alone. All PYP SPECT studies performed at BWH were over read by a single experienced reader (SD) and visual grade was ascertained. For the PYP scans from the two other centers, the clinical interpretation of the visual grade was used, the H:CL ratio was adjunctive.

Study groups

ATTR-CM diagnosis was based on a positive Tc-99m-PYP scan in most cases. A monoclonal gammopathy by free-light chain assay and immunofixation electrophoresis of the serum and urine was an exclusion criterion for the study. In the setting of an abnormal free-light chain assay and/or immunofixation electrophoresis, when an endomyocardial biopsy was available to confirm a diagnosis ATTR-CM (using immunohistochemistry or mass spectrometry) the subjects were included (n=30). Subjects not meeting above criteria were considered non-ATTR-CM.

Echocardiographic analysis

Echocardiograms were performed clinically using commercially available scanners with transducer frequencies appropriate for body size and acoustic windows (iE33, Philips Medical Systems; and Vivid 7, GE Medical Systems, Milwaukee, WI). Echocardiograms from all 3 centers were analyzed at BWH by two experienced observers (SM and SC) as per the most recent American Society of Echocardiography/European Association of Cardiovascular Imaging Guides (ASE/EACVI) (Supplemental material) to include standard measures of cardiac structure, systolic, and diastolic function. The mitral inflow A-wave velocity was not measurable in 240 subjects, predominantly due to the presence of an atrial arrhythmia.

Longitudinal strain

Longitudinal strain was evaluated by a single experienced observer SC from the three apical long-axis views (4-, 2-, 3-chamber views) using speckle-tracking method estimated by a commercially available software validated for this purpose (Image Arena 4.6; TomTec, Unterschleissheim, Germany).[9] The endocardial border was traced at the end-diastolic frame

in the apical views. End diastole was considered as the first frame when the mitral valve was closed[10]. The software tracked speckles along the endocardial and epicardial borders throughout the cardiac cycle, and the width of the region of interest was adjusted to fit the entire myocardium. The results of peak strain estimate were evaluated in 16 segments, 6 segments at the base and mid LV, and 4 segments at the apex of the LV.[11] This was evaluable in 517 subjects (93.5% with ATTR-CMP) (Supplemental material Table S1).

The software generated values for the endocardial border: the inner contour of the myocardium; epicardial border: the outer contour of the myocardium; and the myocardial mid-wall: the middle ROI axis defined in the middle between inner and outer ROI contours. We chose mid-wall values for our analysis. Established strain-derived variables were calculated; septal peak LS apical to basal segment ratio (SAB) using 4 chamber view values[4]; relative apical sparing of global LS ratio (RELAS), the average apical segment peak LS/average basal and mid peak LS using all chambers[3]; ejection fraction to global LS ratio (EFSR)[5]. Published cut-offs for detecting CA are >2.1 for SAB, >1 for RELAS, >4.1 for EFSR.[3–5]

Multiparametric scores

The increased wall thickness (IWT) score was derived from a population of patients with increased wall thickness and suspected cardiac amyloidosis, both immunoglobulin light chain (AL) and ATTR referred to 3 European centers[6]. The score includes relative wall thickness, E/e' ratio, LS, tricuspid annulus planar systolic excursion (TAPSE) and septal apical–to–basal LS ratio (SAB) (Figure 2). Of note, in this score only 4 chamber LS data were used. The IWT score calculation requires a recording of an M-mode image through the tricuspid annulus to calculate TAPSE. We were able to calculate this score from the data from 2 of the 3 sites.

The TCAS score was derived from a sample of patients referred to the Mayo clinic between 2013 and 2020 with HFpEF (EF ≥40%)[8]. It was also validated in an external sample from Northwestern University, Chicago, Illinois. This includes age, sex, relative wall thickness, posterior wall diameter, EF, and history of hypertension (Figure 2). The Mayo TCAS score was calculated for the entire cohort with available parameters (Figure 1).

LASSO binary logistic regression modelling to predict ATTR-CM

A training dataset with 173 patients was used, taken from the BWH cohort. A set of clinically important variables were selected a priori based on prior reports of predictive value in identifying ATTR-CM, which included the following: age; chamber dimensions and volumes, both 4 chamber, 2 chamber and biplane measurements were used for LV and LA volumes; diastolic parameters; LS parameters: average of basal segments, average of mid segments, average of apical segments, global LS, RELAS, 4 chamber LS.

The E/A, A and LA volume were removed for having greater than 15% missing observations. Variables with high collinearity were also removed. Least absolute shrinkage and selection operator (LASSO) was used when fitting the binary logistic regression model to reduce the effects of overfitting and force a subset of variables to have regression coefficients of zero. Since predictor coefficients values can be shrunk fully to zero this

acts as a form of feature selection, potentially removing predictors that capture redundant information, resulting in a simpler and more interpretable models that incorporate only a reduced set of the predictors, for better prediction and model interpretation. One thousand repeats of 10-fold cross validation were used to choose a penalty value for fitting with LASSO. To evaluate this model, the AUC was calculated by applying 10-fold cross validation to the above penalty selection process then repeating this procedure 10 times and taking the mean AUC across these 10 repeats. (Further detail in Supplemental material). We then validated this model using the remaining subjects in the cohort (n=425).

For each echo parameter, a ROC curve with true ATTR-CM as the binary response was created using the initial training dataset (n = 173). The AUC and Youden's index threshold were calculated using each ROC curve; additionally, the sensitivity, specificity, negative predictive value (NPV) and positive predictive value (PPV) were calculated using the Youden's index cut-off for dichotomization. Confidence intervals (95%) were calculated for the AUC using the DeLong method, for Youden's index using the stratified percentile bootstrap (10,000 bootstrap samples), and for sensitivity, specificity, PPV, and NPV using the exact Clopper-Pearson method.

Statistical analysis

Continuous variables are shown as mean ± standard deviation (SD) or median [interquartile range (IQR)] for normally and non-normally distributed data, respectively. Comparisons between 2 groups were performed with two-independent-samples t-tests for data with approximately normal distributions and the Wilcoxon rank-sum tests otherwise. The Pearson's chi-squared and Fisher's exact tests were used to test for differences in categorical data. Receiver operating characteristic (ROC) curve analysis and area under curve (AUC) were used to evaluate the performance for identifying subjects with ATTR-CM, comparison of parameter and model ROCs was performed as outlined above. Categorical net reclassification index (NRI) was calculated using a binary outcome of a positive or negative diagnosis (Supplemental material Table S2). All statistical tests were two-tailed, with p-values < 0.05 considered statistically significant. Analyses were performed using Stata (StataCorp. 2015. Stata Statistical Software: Release 14. College Station, TX: StataCorp LP.) and R (version 4.0.2); R packages *caret*[12], *glmnet*[13], and *pROC*[14] were used.

RESULTS

Characteristics

The study population was predominantly male (78.1%), with a median age of 76 years (interquartile range 70–81 years) (Table 1). Of the 324 patients with ATTR-CM, there were 52 subjects with the V122I mutation, remainder had wild-type ATTR. A history of atrial fibrillation was recorded in over half the population (57.2%). The N-terminal pro-brain natriuretic peptide (NT-proBNP) levels were higher in the ATTR-CM group, despite a higher proportion of the non-ATTR-CM group having New York Heart Association (NYHA) class III and IV symptoms.

Echo parameters

Echo parameters showed certain characteristic differences between the study groups (Table 2). The LV wall thickness and LV mass were higher in the ATTR-CM group (Table 2, p<0.001). The LV EF was lower in patients with ATTR-CM (48.2 ± 11.7% vs 51.5 ± 12.5%, p<0.001). Just over half of the subjects with ATTR-CM had an LV EF of 50% or greater; 21.5% had an LV EF of 40–49%, 17.2% an LV EF of 30–39%, and 7.1% an LV EF<30%. In those with an LV EF of 50% or greater, the myocardial contraction fraction (MCF) was significantly lower in ATTR-CM (0.18 ± 0.09 vs 0.32 ± 0.16, p<0.001).

Diastolic dysfunction was present in 79% of the entire study cohort. The early mitral tissue Doppler velocity (e') was reduced in both groups and lower in the ATTR-CM group (Table 2). Majority of the ATTR-CM group had severely reduced mitral annular tissue Doppler velocities, 84.3% with septal e' ≤ 5 cm/s and 53.7% with lateral e' ≤ 5 cm/s. The other tissue Doppler indices, a' and s', were also lower in the ATTR-CM group (a' 4.3 ± 0.2 cm/s v's 6.8 ± 0.3, p<0.001; s' 4.2 ± 0.1 vs 6.4 ± 0.3, p<0.001).

The mean LA size was enlarged in both groups, without a significant between group difference. Notably, 20% of subjects in the ATTR-CM group had a normal LA diameter (< 40 mm) and 18% had a normal LA indexed volume (< 34 ml/m2).

The RV systolic function was reduced in the ATTR-CM cohort with a mean RV s' of 8.8± 2.8 cm/s versus 10.6 ± 3.4 cm/s, p <0.001. TAPSE was measurable in 226 subjects with ATTR-CM and was reduced at 13.6 ± 5.0 mm.

Longitudinal strain analysis

The global LS was reduced for the entire cohort, but lower in the ATTR-CM group, −8.0 ± 3.0% v's −10.9 ± 4.6%, p<0.001. The difference was more notable when comparing basal and mid-ventricular average LS values (Figure 3 & Table 3), in keeping with the known apical sparing pattern seen in ATTR-CM.

Strain ratios and multiparametric scores

The LS ratios, SAB, RELAS and EFSR, were higher in the ATTR-CM cohort (Figure 3). The published cut-off for RELAS of >1 was met in 7% with ATTR-CM, correctly classifying 42.3%; 74% met the published SAB cut-off of >2.1, correctly classifying 70%; the EFSR cut-off of >4.1 was met by 83.2% of the ATTR-CM group, correctly classifying 66.7% (Table 4). The multiparametric IWT score had an AUC of 0.77 (95% CI: 0.70, 0.82) (Figure 4 & Table 5). The TCAS multiparametric score showed an AUC of 0.83 (95% CI: 0.79, 0.87) (Figure 5 & Table 5). However, there was no distinct cut-off that offered both high sensitivity and specificity (Table 5).

LASSO binary logistic regression for presence of ATTR-CM

Using a LASSO binary logistic regression model in the training dataset (n=173, 65.9% ATTR-CM) the combination of age, inferolateral wall thickness, and mid-wall basal LS was selected and had a cross-validated AUC of 0.90; when applied to the validation set (n=425, 49.6% ATTR-CM) the AUC was 0.87 (95% confidence interval (CI): 0.83, 0.90)

(Supplemental Material Figure S1). The optimal age threshold was 66 years old, with a sensitivity of 96.9%, a specificity of 24.45%, correctly classifying 63.71% of the cohort. Optimal cut-offs inferolateral wall thickness and average basal LS were ≥14 mm and ≥−8%, respectively, based on number of patients correctly classified (Table 5).

Comparison of individual parameters, ratios, scores

We compared the AUCs for detecting ATTR-CM of the stand-alone echo parameters from our regression model with the strain ratios and multiparametric scores. Although ROC curves using continuous variables are optimal, binary cutoff values for the measurements, ratios and scores are often used in the clinical practice. Hence, we evaluated both continuous values (Figures 5A and B) and binary cut off values (Figures 5C and D). The inferolateral wall thickness cut-off of ≥14 mm (AUC 0.72, CI: 0.68–0.76) outperformed RELAS >1 (AUC 0.53, CI: 0.51–0.54, p<0.001), EFSR>4.1 (AUC 0.63, CI: 0.59–0.67, p<0.001); it was equivalent to SAB >2.1 (AUC 0.69, CI: 0.64–0.73, p=0.1) and the proposed cut-off of 6 for TCAS (AUC 0.72, CI: 0.68–0.75, p=0.8) (Figure 5A). Findings were similar for an average basal LS ≥−8% (AUC: 0.76, CI: 0.72–0.79); which outperformed RELAS >1 (p<0.001), EFSR>4.1 (p<0.001) and SAB >2.1 (p=0.01), but was equivalent to TCAS >6 (p=0.2) (Figure 5B). The IWT score was only calculated in data from two of the sites (n=307). There was no significant difference between inferolateral wall thickness and IWT score AUC (p=0.4), whereas the AUC for basal LS was significantly higher (p=0.04).

Discussion

We evaluated the accuracy of echocardiographic features to diagnose ATTR-CM by Tc-99m-PYP scintigraphy in a large three-center cohort of 598 patients with suspected ATTR-CM using a central core lab-based analysis of echocardiograms. Our goals were to develop a predictive model for ATTR-CM using echocardiographic measures and to externally validate and compare the diagnostic accuracy of previously defined LS ratios and multiparametric echo scores. The notable findings of our study were that age, inferolateral wall thickness, and the average basal LS value best predicted ATTR-CM with high accuracy (AUC 0.90 in training set, 0.87 in the validation set). Remarkably, simple measures of the average basal LS and the inferolateral wall thickness performed as well as more complex multiparametric TCAS score and the SAB ratio to diagnose ATTR-CM by Tc-99m-PYP scintigraphy.

Apical sparing ratios

Apical sparing of LS is a known feature of ATTR-CM. The SAB and RELAS ratios quantify this phenomenon. The published cut-off for SAB of >2.1 correctly classified 70%, the RELAS cut-off of >1 correctly classified 57.8% of subjects, but had a high specificity, 99% vs 64% for SAB. There are several factors to explain the underperformance of these ratios in our study cohort compared to the originally published AUC of 0.91 and 0.94, for SAB and RELAS respectively. Both these ratios were developed in selected cohorts with cardiac amyloidosis, hypertrophic cardiomyopathy, aortic stenosis, or isolated arterial hypertension, Fabry disease, Friedreich ataxia and healthy volunteers[3,4]; limiting their application to more heterogeneous HFpEF populations. Our findings were similar to those of Pagourelias et

al, they found that RELAS and SAB has AUCs of 0.78 and 0.67 in their analysis of 100 patients with increased wall thickness (40 with Cardiac Amyloidosis, 40 with HCM and 20 with hypertension)[5]. Secondly, one of the known limitations of strain analysis is variation in LS between vendors. These ratios were originally developed using the GE EchoPAC platform[3–6]. The intervendor variation and its impact on the RELAS threshold of >1 has previously been evaluated by Sperry et al.[15] They found a mean RELAS < 1 comparing vendors; GE (EchoPAC), Siemens (Velocity Vector Imaging), and Phillips (QLab) systems. The TomTec platform was not assessed in that study. It is one of the few vendor neutral platforms, hence, frequently used in large echocardiographic core laboratories[16,17]. The software platform used is an important consideration when applying strain ratios or the IWT score, which includes SAB, to clinical trial data to assess for potential cardiac amyloidosis[18,19]. The TomTec platform also allows layer specific analysis, the myocardial layer (endo versus mid. versus epicardial layer) chosen can significantly alter the LS value. Our data suggests that when using the TomTec platform a reduced average basal LS is more predictive than an apical sparing ratio.

Potential Value of Multiparametric Scores

A highly predictive multiparametric echo score for detecting ATTR-CM could have great potential for clinical use in selecting patients for evaluation of ATTR-CM and for risk assessment. The interest in a multiparametric approach is evident with the recent publication of two multiparametric scores from large referral centers. However, caution is needed when using these metrics to exclude ATTR-CM. The population we evaluated was enriched for ATTR-CM as a clinical suspicion for the disease lead to referral for Tc-99m-PYP. Our data suggest that the Mayo Clinic derived TCAS multiparametric score can identify patients most likely to benefit from further evaluation with Tc-99m-PYP scans, but this score does not have a single cut-off that offers both high sensitivity and specificity. The same is true for the European IWT score, hence, neither are particularly helpful to rule-out disease if there is a clinical suspicion. At any given cut-off the diagnostic performance of these echo scores in predicting ATTR-CM remained only modest (Table 5). This also limits the utility of these scores in retrospective ad-hoc analyses to identify possible cardiac amyloidosis patients in negative HFpEF trials[18,19].

ATTR-CM disease stage is another key factor to consider when developing and applying any diagnostic criteria. If diagnostic criteria rely on presence of more advanced features of the disease, early disease may be missed. With the broader use of cardiac scintigraphy, patients are being screened for amyloidosis at earlier stages of the disease, and it is likely that currently referred patients will not have the same degree of wall thickness, diastolic dysfunction or strain abnormalities traditionally associated with cardiac amyloidosis. This further enforces our observation that using thresholds developed in populations with distinct etiologies of increased LV wall thickness may be less reliable, instead attention should be paid to the pattern of strain rather than absolute values of ratios.

Limitations

This large 3-center study has several limitations. All three centers are academic and urban centers with extensive experience and a referral amyloid cohort. We used clinically acquired

echocardiograms and retrospective chart review, hence, there were missing data points. These was addressed through imputation, but in the case of TAPSE we only analyzed the IWT in data from 2 sites. Many of the prior publications used highly selected cohorts with increased ventricular wall thickness, sometimes combining AL and ATTR patients.[3–5] We chose a sample with clinically suspected ATTR-CM, making the results clinically relevant. However, as with prior studies, this study is still a population referred to major urban academic centers with extensive expertise in amyloidosis. In non-academic, non-referral center cohorts, the pretest probability of ATTR-CM may be lower reducing the yield of the Tc-99m-PYP scans. Hence, a prospective study of a broader population is required to validate the most useful parameters in clinical practice. As this study focused on ATTR-CM, these results are most applicable to patients with suspected ATTR cardiac amyloidosis. We did not integrate past medical history or ECG features in our models, as we set out to find metrics that can be used by the echocardiographer at time of interpretation of the echocardiogram without needing to access additional medical information.

CONCLUSIONS

As more patients are screened for ATTR-CM, echocardiographic features are essential to aid detection of disease and improve patient selection for referral toTc-99m-PYP SPECT. Several deformation-based ratios and multiparametric scores have been proposed to improve the echocardiographic detection of ATTR-CM. However, in this population with suspected cardiac amyloidosis increased inferolateral wall thickness and a reduced basal average LS were robust predictors of ATTR-CM and outperformed many of these more complex ratios and scores.

Supplementary Material

Refer to Web version on PubMed Central for supplementary material.

SOURCES OF FUNDING:

This work was supported by a research grant from the Pfizer APSIRE program to Dr. S.A.M. Cuddy.

DISCLOSURES

SAMC: Honoria from BridgeBio, Pfizer, Ionis, Guidepoint. Research funding from Pfizer.

MM: is supported by the NIH (grants R01HL139671-01, R21AG058348 and K24AG036778). Has received consulting fees from Pfizer, GlaxoSmithKline, EIdos, Prothena, Akcea, and Alnylam; and has received clinical trial funding from Pfizer, Prothena, Eidos, and Alnylam

FR: is supported by the National Institutes of Health (NIH) (grants HL139671-01 and AG 050206-02).Has received support from Eidos Therapeutics; and has received consulting fees from Pfizer and GlaxoSmithKline.

RHF: has received consulting fees from Ionis Pharmaceuticals, Alnylam Pharmaceuticals, and Caelum Biosciences; and has received research funding from GlaxoSmithKline, Eidos, Akcea, and Pfizer.

SD: supported by grants from the National Institutes of Health (R01 HL 150342; K24 HL 157648), Pfizer, Phillips, GE Healthcare and Attrallus and and has received consulting fees/honoraria from Janssec and Ionetix.

Abbreviations:

AL	light-chain amyloidosis
ATTR	transthyretin amyloidosis
ATTR-CM	transthyretin amyloid cardiomyopathy
EFSR	ejection fraction to global longitudinal strain
hATTR	hereditary (genetically abnormal) transthyretin amyloidosis
HF	heart failure
HFpEF	heart failure with preserved ejection fraction
IWT	increased wall thickness score
LS	longitudinal strain
RELAS	relative apical sparing ratio
SAB	septal apex to base ratio
TCAS	transthyretin cardiac amyloidosis score
Tc-99m-PYP	technetium-99m pyrophosphate scintigraphy
TTR	transthyretin
wtATTR	wild-type (genetically normal) transthyretin amyloidosis

REFERENCES

1. Gillmore JD, Maurer MS, Falk RH, Merlini G, Damy T, Dispenzieri A, Wechalekar AD, Berk JL, Quarta CC, Grogan M,et al. Nonbiopsy diagnosis of cardiac transthyretin amyloidosis. Circulation. 2016;133:2404–2412. doi:10.1161/CIRCULATIONAHA.116.021612 [PubMed: 27143678]
2. Knight DS, Zumbo G, Barcella W, Steeden JA, Muthurangu V, Martinez-Naharro A, Treibel TA, Abdel-Gadir A, Bulluck H, Kotecha T, et al. Cardiac Structural and Functional Consequences of Amyloid Deposition by Cardiac Magnetic Resonance and Echocardiography and Their Prognostic Roles. JACC Cardiovasc Imaging. 2019;12:823–33. doi:10.1016/j.jcmg.2018.02.016 [PubMed: 29680336]
3. Phelan D, Collier P, Thavendiranathan P, Popovi ZB, Hanna M, Plana JC, Marwick TC, Thomas JD. Relative apical sparing of longitudinal strain using two-dimensional speckle-tracking echocardiography is both sensitive and specific for the diagnosis of cardiac amyloidosis. Heart. 2012;98:1442–1448. doi:10.1136/heartjnl-2012-302353 [PubMed: 22865865]
4. Liu D, Hu K, Niemann M, Herrmann S, Cikes M, Störk S, Gaudron PD, Knop S, Ertl G, Bijnens B, et al. Effect of combined systolic and diastolic functional parameter assessment for differentiation of cardiac amyloidosis from other causes of concentric left ventricular hypertrophy. Circ Cardiovasc Imaging. 2013;6:1066–1072. doi:10.1161/CIRCIMAGING.113.000683 [PubMed: 24100046]
5. Pagourelias ED, Mirea O, Duchenne J, Van Cleemput J, Delforge M, Bogaert J, Kuznetsova T, & Voig JU. Echo Parameters for Differential Diagnosis in Cardiac Amyloidosis: A Head-to-Head Comparison of Deformation and Nondeformation Parameters. Circ Cardiovasc Imaging. 2017;10:e005588. doi:10.1161/CIRCIMAGING.116.005588 [PubMed: 28298286]
6. Boldrini M, Cappelli F, Chacko L, Restrepo-Cordoba MA, Lopez-Sainz A, Giannoni A, Aimo A, Baggiano A, Martinez-Naharro A, Whelan C, et al. Multiparametric Echocardiography Scores for

the Diagnosis of Cardiac Amyloidosis. JACC Cardiovasc Imaging. 2020;13:909–920. doi:10.1016/j.jcmg.2019.10.011 [PubMed: 31864973]

7. Davies DR, Redfield MM, Scott CG, Minamisawa M, Grogan M, Dispenzieri A, Chareonthaitawee P, Shah AM, Shah SJ, Wehbe R, et al. A Simple Score to Identify Increased Risk of Transthyretin Amyloid Cardiomyopathy in Heart Failure With Preserved Ejection Fraction. JAMA Cardiol. Published online September 07, 2022. doi:10.1001/jamacardio.2022.1781
8. Haq M, Pawar S, Berk JL, Miller EJ, Ruberg FL. Can 99mTc-Pyrophosphate Aid in Early Detection of Cardiac Involvement in Asymptomatic Variant TTR Amyloidosis? JACC Cardiovasc Imaging. 2017;10:713–714. doi:10.1016/j.jcmg.2016.06.003 [PubMed: 27568122]
9. Lang RM, Badano LP, Mor-Avi V, Afilalo J, Armstrong A, Ernande L, Flachskampf FA, Foster E, Goldstein SA, Kuznetsova T, Lancellotti P,et al. Recommendations for cardiac chamber quantification by echocardiography in adults: an update from the American Society of Echocardiography and the European Association of Cardiovascular Imaging. J Am Soc Echocardiogr. 2015;28:1–39.e14. doi:10.1016/j.echo.2014.10.003 [PubMed: 25559473]
10. Mada RO, Lysyansky P, Daraban AM, Duchenne J, Voigt J-U. How to Define End-Diastole and End-Systole? Impact of Timing on Strain Measurements. JACC: Cardiovascular Imaging. 2015;8:148–57. [PubMed: 25577447]
11. Ünlü S, Mirea O, Duchenne J, Pagourelias ED, Bézy S, Thomas JD, Badano LP, Voigt JU. Comparison of Feasibility, Accuracy, and Reproducibility of Layer-Specific Global Longitudinal Strain Measurements Among Five Different Vendors: A Report from the EACVI-ASE Strain Standardization Task Force. J Am Soc Echocardiogr. 2018;31:374–380.e1. doi:10.1016/j.echo.2017.11.008 [PubMed: 29246512]
12. Kuhn M, Wing J, Weston S, Williams A, Keefer C, Engelhardt A, Cooper T, Mayer Z, Kenkel B. caret: Classification and Regression Training. R package version 6.0-86. Astrophysics Source Code Library: Cambridge, MA, USA (2020).
13. Friedman J, Hastie T, Tibshirani R. Regularization paths for generalized linear models via coordinate descent. J Stat Softw. 2010;33:1–22. doi:10.18637/jss.v033.i01 [PubMed: 20808728]
14. Robin X, Turck N, Hainard A, Tiberti N, Lisacek F, Sanchez JC, Müller M. pROC: An open-source package for R and S+ to analyze and compare ROC curves. BMC Bioinformatics. 2011;12:1–8. doi:10.1186/1471-2105-12-77 [PubMed: 21199577]
15. Sperry BW, Sato K, Phelan D, Grimm R, Desai MY, Hanna M, Jaber WA, Popović ZB. Regional variability in longitudinal strain across vendors in patients with cardiomyopathy due to increased left ventricular wall thickness. Circ Cardiovasc Imaging. 2019;12:1–10. doi:10.1161/CIRCIMAGING.119.008973
16. Shah AM, Cikes M, Prasad N, Li G, Getchevski S, Claggett B, Rizkala A, Lukashevich I, O'Meara E, Ryan JJ, Shah SJ, et al. Echocardiographic Features of Patients With Heart Failure and Preserved Left Ventricular Ejection Fraction. J Am Coll Cardiol. 2019;74:2858–2873. doi:10.1016/j.jacc.2019.09.063 [PubMed: 31806129]
17. Minamisawa M, Claggett B, Adams D, Kristen AV, Merlini G, Slama MS, Dispenzieri A, Shah AM, Falk RH, Karsten V, et al. Association of Patisiran, an RNA Interference Therapeutic, with Regional Left Ventricular Myocardial Strain in Hereditary Transthyretin Amyloidosis: The APOLLO Study. JAMA Cardiol. 2019;4:466–472. doi:10.1001/jamacardio.2019.0849 [PubMed: 30878017]
18. Sperry BW, Hanna M, Shah SJ, Jaber WA, Spertus JA. Spironolactone in Patients With an Echocardiographic HFpEF Phenotype Suggestive of Cardiac Amyloidosis. JACC Hear Fail. 2021;9:795–802. doi:10.1016/j.jchf.2021.06.007
19. Oghina S, Bougouin W, Bézard M, Kharoubi M, Komajda M, Cohen-Solal A, Mebazaa A, Damy T, Bodez D. The Impact of Patients With Cardiac Amyloidosis in HFpEF Trials. JACC Hear Fail. 2021;9:169–178. doi:10.1016/j.jchf.2020.12.005

CLINICAL PERSPECTIVE:

Cardiac amyloidosis due to transthyretin amyloidosis (ATTR-CM) is an under-appreciated disease. ATTR-CM has typical features on echocardiography, including relative sparing of the longitudinal strain of the apical segments. To aid the detection of ATTR-CM, several strain-based ratios have been devised and are purported to have high sensitivity and specificity. More recently multi-parametric scores that incorporate echocardiographic features have been developed. We examined the echocardiographic features of a population of patients with suspected ATTR-CM referred for cardiac scintigraphy with technetium 99m labeled pyrophosphate (PYP) and assessed the diagnostic accuracy of previously published strain ratios and multiparametric scores. We showed that an increased inferolateral wall thickness ≥ 14 mm or reduced basal longitudinal strain ≥−8% performed as well or better than the various strain ratios and echocardiographic scores. With increased availability of cardiac scintigraphy for the screening and diagnosis of ATTR-CM, using stand-alone echo parameters to help identify patients at increased risk of ATTR-CM is a more straightforward approach than calculation of ratios or scores.

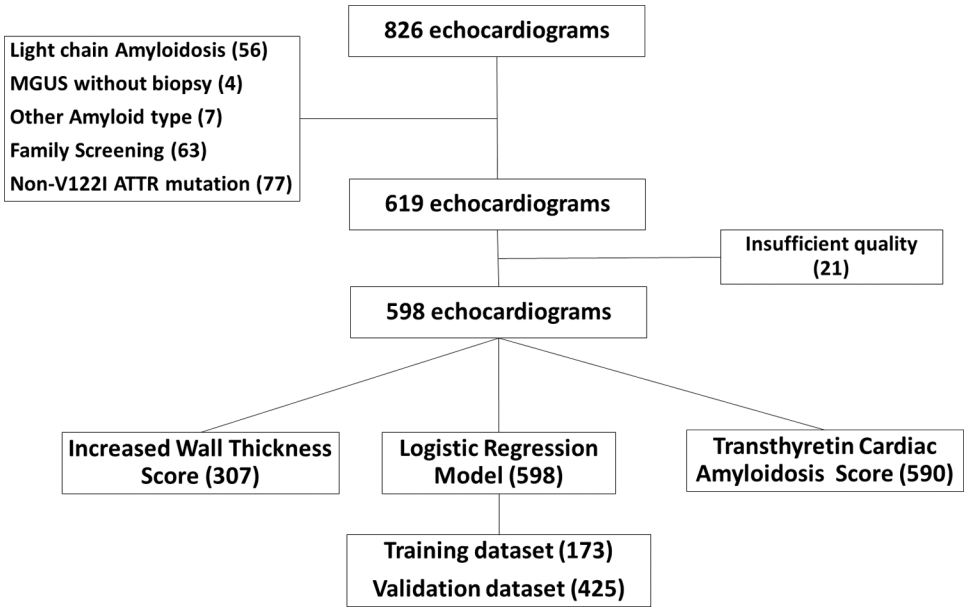

Figure 1: CONSORT Diagram.

A

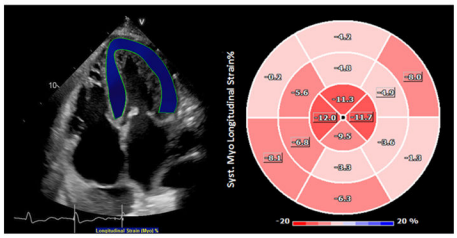

B

$$\text{RELAS} = \frac{\text{Average Apical LS}}{\text{Sum of average Base and Mid LS}}$$

$$\text{SAB} = \frac{\text{Apical Septal (4C) LS}}{\text{Basal Septal (4C) LS}}$$

$$\text{EFSR} = \frac{\text{LV EF}}{\text{GLS}}$$

C

Increased Wall Thickness Score		
Parameter	Cut-Off	Points
Relative WT	>0.6	3
E/e'	>11	1
TAPSE, mm	≤19	2
LS (4-chamber), %	≥-13	1
SAB	>2.9	3
LS, longitudinal strain; SAB, septal apical to base ratio; TAPSE, tricuspid annular plane systolic excursion; WT, wall thickness.		

D

Transthyretin Cardiac Amyloidosis Score		
Parameter	Cut-Off	Points
Age, years	60-69 70-79 ≥ 80	+2 +3 +4
Sex	Male	+2
Relative WT	>0.57	+2
Inferolateral WT, mm	≥12	+1
LV EF, %	<60	+1
Hypertension diagnosis	Present	-1
LV EF, left ventricular ejection fraction; WT, wall thickness		

Figure 2: Longitudinal strain-based ratios and multi-parametric scores to aid detection of cardiac amyloidosis.

Panel A shows a region of interest for the calculation of LS in the apical 4-chamber view, with the polar plot showing apical sparing of LS. Panels B displays the various strain-based ratios. Panels C and D (Tables) display the calculations for the Increased Wall Thickness score and the Transthyretin Cardiac Amyloidosis Score (TCAS).

EFSR, ejection fraction strain ratio; LS, longitudinal strain; LV EF, left ventricular ejection fraction; RELAS, relative apical sparing ratio; RWT, relative wall thickness; SAB, septal apical to base ratio; TAPSE, tricuspid annular plane systolic excursion.

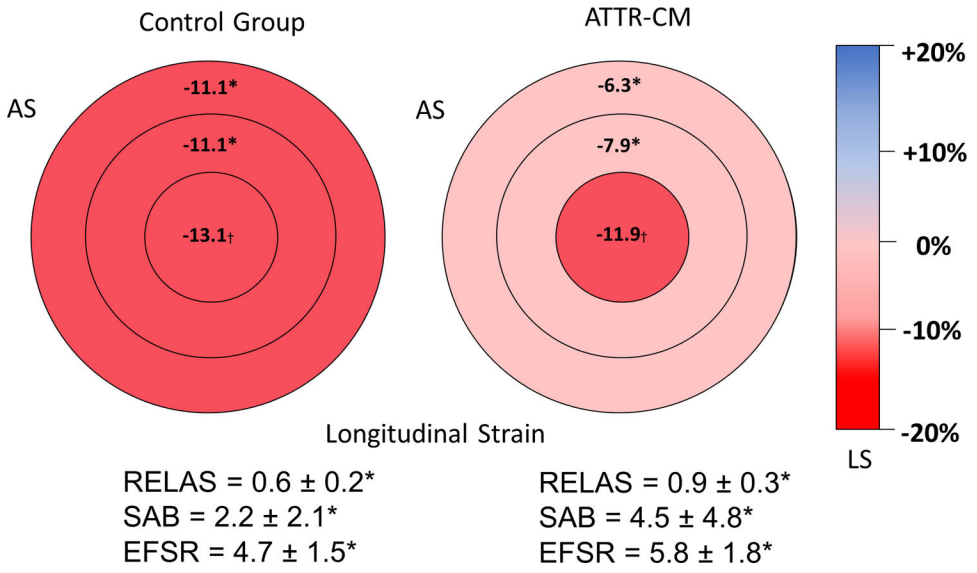

Figure 3: Left ventricular bullseye plots showing the longitudinal strain values of the base, mid and apical segments.

AS, anteroseptum; ATTR-CM, transthyretin amyloidosis cardiomyopathy; EFSR, ejection fraction strain ratio; LS, longitudinal strain; RELAS, relative apical sparing ratio; SAB, septal apex base ratio. * $p<0.001$. † $p=0.004$

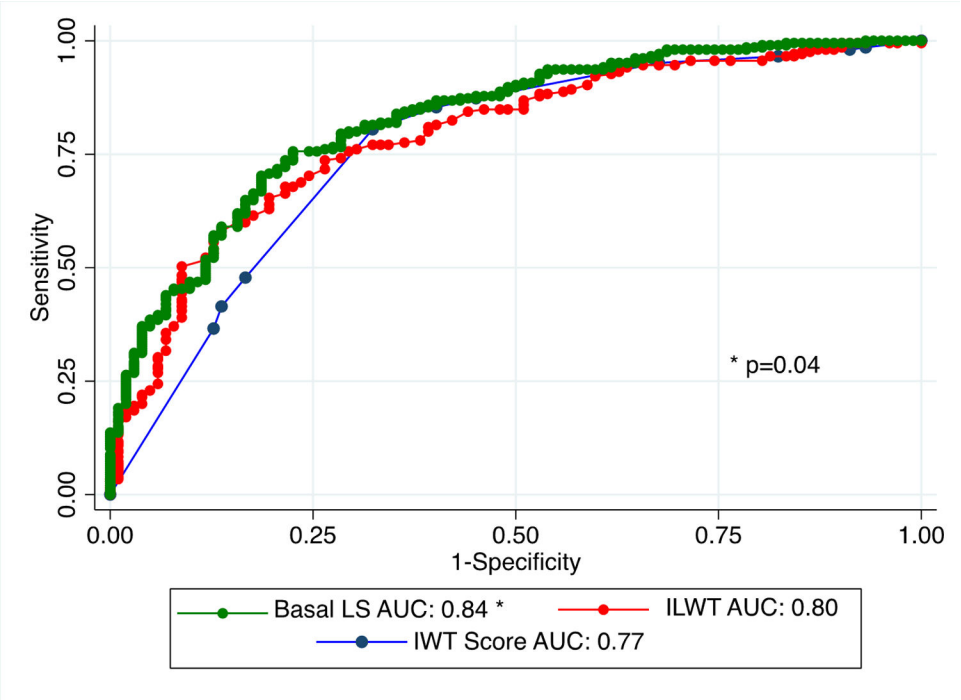

Figure 4: Comparison of receiver operating characteristic curves for the diagnosis of cardiac transthyretin amyloidosis with increased wall thickness score

Comparison of receiver operating characteristic curves of inferolateral wall thickness and average basal LS with increased wall thickness score. The AUC are statistically significant when noted with *.

AUC, area under the curve; ILWT, inferolateral wall thickness; IWT, increased wall thickness score; LS, longitudinal strain.

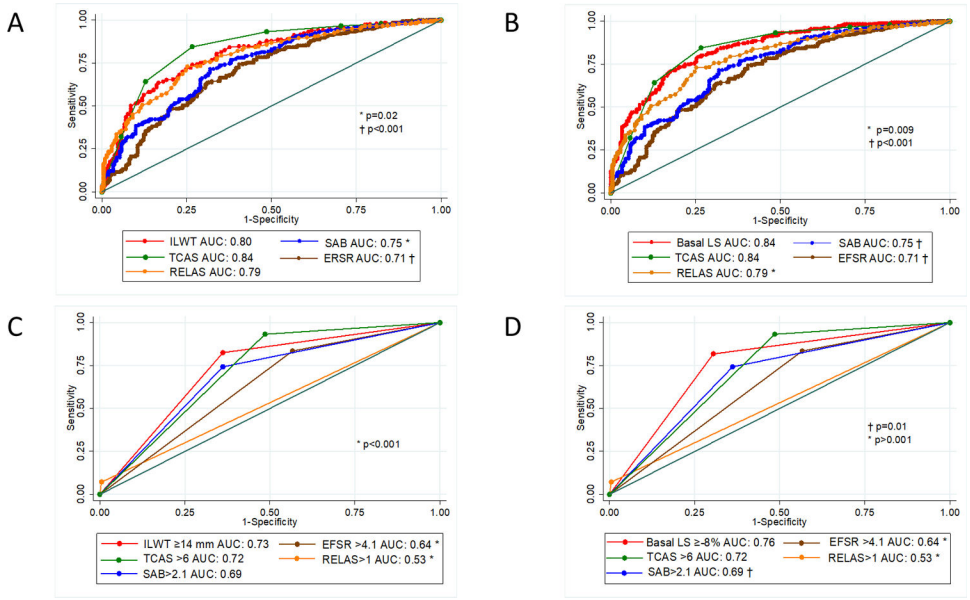

Figure 5: Comparison of receiver operating characteristic curves to diagnose cardiac transthyretin amyloidosis with continuous variable and specific cut-offs.

Comparison of receiver operating characteristic curves of A) inferolateral wall thickness and B) average basal LS to deformation ratios (RELAS, SAB, EFSR) and the TCAS multiparametric score to diagnose cardiac transthyretin amyloidosis. C) & D) are receiver operating characteristic curves using specified cut-offs for each parameter. The AUC are statistically significant when noted with * or **.

AUC, area under the curve; EFSR, ejection fraction to strain ratio; ILWT, inferolateral wall thickness; LS, longitudinal strain; RELAS, relative apical sparing ratio; SAB, septal apical to base LS ratio; TCAS, Mayo clinic derived ATTR score.

Table 1:

Patient characteristics

Characteristic	No ATTR-CM (n=274)	ATTR-CM (n=324)	p-value
Male	186 (67.6%)	283 (87.1%)	<0.001
Age, years	68.5 [59.5, 79.5]	76.0 [71.0, 81.0]	0.002
BSA, m ^{2}	2.0 ± 0.3	2.0 ± 0.2	0.65
Race			0.019
Unknown	49 (17.9%)	85 (26.2%)	
Black	60 (21.9%)	55 (17.0%)	
White	159 (58.0%)	169 (52.2%)	
Other	6 (2.2 %)	15 (4.6 %)	
V122I	0 (0.0 %)	52 (16%)	<0.001
A Fib	136 (50.6%)	201 (62.8%)	0.002
HTN	230 (84.6%)	219 (68.9%)	<0.001
HLD	169 (62.4%)	177 (55.5%)	0.09
CAD	82 (30.1%)	68 (21.3%)	0.003
TAVR/TAVI	8.6%	2.1%	0.001
NYHA Class			0.003
I	45 (19.9%)	57 (19.7%)	
II	62 (27.4%)	117 (40.5%)	
III	95 (41.9%)	100 (34.6%)	
IV	24 (10.6%)	15 (5.2%)	
NT proBNP (pg/L)	1856.5 [784.0, 6036.0]	2721.0 [1456.0, 5723.0]	0.006
eGFR (MDRD)	51.3±24.8	55.6±19.5	0.02
Tc-99m-PYP Grade			<0.001
0	191 (69.7%)	0 (0.0 %)	
1	83 (30.3%)	0 (0.0 %)	
2	0 (0.0 %)	43 (13.3%)	
3	0 (0.0 %)	281 (86.7%)	

A Fib, atrial fibrillation; BSA, body surface area; CAD, coronary artery disease; eGFR, estimated glomerular filtration rate; HLD, hyperlipidaemia; HTN, hypertension; MDRD, Modification of Diet in Renal Disease; NYHA, New York Heart Association; PYP, pyrophosphate.

Data is displayed as mean ± standard deviation for normally distributed data, median [interquartile range] otherwise.

Table 2.

Echocardiographic parameters in patients with and without ATTR-CM.

Characteristic	No ATTR-CM (n=274)	ATTR-CM (n=324)	p-value
IVS d (mm)	13.8 ± 3.6	17.1± 3.2	<0.001
PW d (mm)	12.6 ± 3.1	16.5 ± 3.4	<0.001
LV ED d (mm)	45.5 ± 8.1	42.0 ± 6.5	<0.001
LV ES d (mm)	32.9 ± 9.1	33.2 ± 7.1	0.64
LA d (mm)	46.0 ± 9.6	45.7 ± 6.5	0.61
LAVI (ml/m2)	47.0 21.1	46.4 13.6	0.76
LV EF (%)	51.5 ± 12.5	48.2 ± 11.7	0.001
LV mass (g)	235.8 ± 80.5	300.0 ± 81.2	<0.001
LV mass index (g/m^2)	119.9 ± 37.9	153.1 ± 37.9	<0.001
E wave (m/s)	0.93 ± 0.32	0.86 ± 0.22	0.003
A wave (m/s) *	0.78 [0.53, 1.0]	0.34 [0.23, 0.56]	<0.001
e' septal (cm/s)	5 [4, 6]	4 [3, 5]	<0.001
e' lateral (cm/s)	7 [5, 9]	5 [4, 7]	<0.001
E/A *	0.96 [0.72, 1.75]	2.1 [1.3, 3.12]	<0.001
E/e'	14.7 [10.6, 20.3]	17.4 [13.9, 22.8]	<0.001
DT (msec)	192 ± 61	183 ± 53	0.03
TAPSE (mm) *	16.0 ± 5.3	13.6 ± 5.0	<0.001
RV s' (cm/s)	10.6 ± 3.4	8.8 ± 2.8	<0.001
TR Vmax (m/s)	2.7 ± 0.6	2.5 ± 0.5	0.01
MCF *	0.32 ± 0.16	0.18 ± 0.09	<0.001
Relative Wall Thickness	0.58 ± 0.20	0.81 ± 0.24	<0.001
Eccent. Ratio	1.06 [0.92, 1.27]	1.02 [0.92, 1.16]	0.01

d, diameter; DT, deceleration time; Eccent., eccentricity; ED, end diastolic; EF, ejection fraction; ES, end systolic; IVS, interventricular septum; LA, left atrial; LV, left ventricular; MCF, myocardial contraction fraction; PW, posterior wall; RV, right ventricular; TR, tricuspid regurgitation; Vmax, maximum velocity.

Data is displayed as mean ± standard deviation for normally distributed data, median [interquartile range] otherwise.

* parameter not measured in entire cohort as detailed in text

Table 3:

Longitudinal strain parameters in patients with and without ATTR-CM

Characteristic	No ATTR-CM (n=214)	ATTR-CM (n=303)	p-value
GLS (%)	−11.6 ± 4.1	−8.4 ± 2.9	<0.001
Basal GLS (%)	−11.1 ± 4.5	−6.3 ± 2.8	<0.001
Mid ventricular GLS (%)	−11.1 ± 4.4	−7.9 ± 3.2	<0.001
Apical GLS (%)	−13.1 ± 5.7	−11.9 ± 4.2	0.004
RELAS	0.6 ± 0.2	0.9 ± 0.3	<0.001
SAB	2.2 ± 2.1	4.5 ± 4.8	<0.001
EFSR	4.7 ± 1.5	5.8 ± 1.8	<0.001

EFSR, ejection fraction strain ratio; GLS, global longitudinal strain; RELAS, relative apical sparing ratio; SAB, septal apical to base longitudinal strain ratio.

Data is displayed as mean ± standard deviation.

*parameter not measured in entire cohort as detailed in text

Table 4:

Receiver Operator Curve Characteristics and Cut-Off Points of Strain Parameters for Diagnosis of ATTR-CM

	SAB	RELAS	EFSR
Cut point	>2.1	>1	>4.1
Sensitivity (%)	74.2	7.3	83.2
Specificity (%)	63.7	99.1	43.4
Correctly Classified (%)	69.8	45.3	66.7
Positive LR	2.04	7.7	1.5
Negative LR	0.41	0.94	0.39
AUC	0.69	0.53	0.63
Standard Error	0.02	0.01	0.02
95% CI	0.65–0.73	0.52–0.55	0.59–0.67

AUC, area under the curve; CI, confidence interval; EFSR, ejection fraction strain ratio; LR, likelihood ratio; RELAS, relative apical sparing ratio; SAB, septal apical to base longitudinal strain ratio.

Table 5:

Diagnostic performance of IWT & TCAS scores for ATTR-CM

IWT Score				TCAS score				Inferolateral Wall Thickness				Basal Longitudinal Strain			
Cut point	**Sensitivity**	**Specificity**	**Correctly Classified**	**Cut point**	**Sensitivity**	**Specificity**	**Correctly Classified**	**Cut-point (mm)**	**Sensitivity**	**Specificity**	**Correctly Classified**	**Cut-point (%)**	**Sensitivity**	**Specificity**	**Correctly Classified**
≥ 0	100.00%	0.00%	66.99%	≥ 0	100.00%	0.00%	51.73%	(≥ 7)	99.69%	0.00%	54.01%	(≥ −20)	100.00%	4.19%	60.31%
≥ 1	98.55%	6.86%	68.28%	≥ 1	100.00%	0.45%	51.95%	(≥ 8)	99.69%	2.55%	55.18%	(≥ −19)	100.00%	5.12%	60.69%
≥ 2	98.07%	8.82%	68.61%	≥ 2	99.58%	3.14%	53.03%	(≥ 9)	99.07%	9.49%	58.03%	(≥ −18)	99.67%	6.51%	61.08%
≥ 3	96.62%	17.65%	70.55%	≥ 3	99.58%	8.97%	55.84%	(≥ 10)	98.15%	17.15%	61.04%	(≥ −17)	99.67%	8.37%	61.85%
≥ 4	95.17%	32.35%	74.43%	≥ 4	98.33%	17.04%	59.09%	(≥ 11)	95.99%	25.91%	63.88%	(≥ −16)	99.34%	12.09%	63.20%
≥ 5	86.96%	54.90%	76.38%	≥ 5	97.49%	28.70%	64.29%	(≥ 12)	92.90%	38.32%	67.89%	(≥ −15)	99.34%	15.35%	64.55%
≥ 6	85.02%	59.80%	76.70%	≥ 6	93.72%	50.22%	72.73%	(≥ 13)	87.35%	50.73%	70.57%	(≥ −14)	99.01%	20.47%	66.47%
≥ 7	80.19%	67.65%	76.05%	≥ 7	83.68%	70.85%	77.49%	(≥ 14) *	81.48%	62.41%	72.74%	(≥ −13	98.36%	25.58%	68.21%
≥ 8	48.31%	84.31%	60.19%	≥ 8	64.85%	85.65%	74.89%	(≥ 15)	73.46%	71.90%	72.74%	(≥ −12)	97.37%	32.56%	70.52%
≥ 9	42.03%	87.25%	56.96%	≥ 9	30.13%	93.27%	60.61%	(≥ 16)	61.42%	83.94%	71.74%	(≥ −11)	95.72%	40.47%	72.83%
≥ 10	37.20%	88.24%	54.05%	≥ 10	5.02%	99.55%	50.65%	(≥ 17)	51.23%	90.88%	69.40%	(≥ −10)	92.76%	49.30%	74.76%
				> 10	0.00%	100.00%	48.27%	(≥ 18)	41.67%	94.16%	65.72%	(≥ −9)	87.50%	58.14%	75.34%
								(≥ 19)	29.94%	95.99%	60.20%	(≥ −8) *	81.91%	68.37%	76.30%
								(≥ 20)	18.83%	97.81%	55.02%	(≥ −7)	73.36%	78.14%	75.34%
								(≥ 21)	11.42%	98.91%	51.51%	(≥ −6)	60.20%	85.12%	70.52%
								(≥ 22)	5.86%	98.91%	48.49%	(≥ −5)	47.04%	92.09%	65.70%

Circ Cardiovasc Imaging. Author manuscript; available in PMC 2023 November 15.

IWT Score				TCAS score				Inferolateral Wall Thickness				Basal Longitudinal Strain			
Cut point	**Sensitivity**	**Specificity**	**Correctly Classified**	**Cut point**	**Sensitivity**	**Specificity**	**Correctly Classified**	**Cut-point (mm)**	**Sensitivity**	**Specificity**	**Correctly Classified**	**Cut-point (%)**	**Sensitivity**	**Specificity**	**Correctly Classified**
								(≥ 23)	3.40%	99.64%	47.49%	(≥ −4)	27.63%	97.21%	56.45%
								(≥ 24)	2.47%	100.00%	47.16%	(≥ −3)	12.83%	100.00%	48.94%

IWT, Increased Wall Thickness; TCAS, Mayo clinic derived Transthyretin Cardiac Amyloidosis score.

*Chosen cut-off